

## IMPROVEMENT OF THE OPTICAL PROPERTIES OF ITO/SiO<sub>2</sub>/GLASS FILMS FOR PHOTOVOLTAIC APPLICATIONS

M. M. ABD EL-RAHEEM<sup>a,c</sup>, H. M. ALI<sup>b,c</sup>, N. M. AL-HOSINY<sup>a</sup>,  
M. S. ABD EL AAL<sup>d</sup>

<sup>a</sup>*Physics Department, Faculty of Science, El-Taef University, Kingdom of Saudi Arabia*

<sup>b</sup>*Physics Department, Faculty of Science, Al-Baha University, Kingdom of Saudi Arabia*

<sup>c</sup>*Physics Department, Faculty of Science, 82524 Sohag, Sohag University, Egypt*

<sup>d</sup>*Spectroscopy Department, National Research Center, Cairo, Egypt*

High-quality ITO thin films were deposited onto different thicknesses of SiO<sub>2</sub> buffer layer by Electron beam deposition technique at different substrate temperatures (200 – 325 °C). The effect of grain size (up to 13.5 nm) on the optical properties leads to decreasing both of reflectance and thermal emissivity and increasing the optical gap with decreasing the grain size of the films respectively. The transmittance values are found to increase with increasing both the thickness of buffer layer and the substrate temperature. An average transmittance value of 92 % in the visible region and 83% in the near infrared (NIR) region of the spectrum and a resistivity value of  $1.6 \times 10^{-4}$  ( $\Omega$  cm) are obtained. An increase in the band gap (3.08-3.54 eV) is observed by increasing the substrate temperature from 200 to 325 °C. The refractive index, extinction coefficient, Kubelka-Munk function and thermal emissivity of the thin films were determined and presented in this work.

(Received February 23, 2010; accepted March 15, 2010)

*Keywords:* ITO/SiO<sub>2</sub> glass; Thin Film; Photovoltaic; Optical properties

### 1. Introduction

Transparent conducting (TCO) films are frequently used in numerous applications such as optoelectronic devices, surface acoustic wave devices, gas sensors, ferroelectric photo-conductor storage devices antistatic coatings, light-emitting, light detecting, thin film transistors and light-triggered semiconductor devices, electrodes for electrochromic devices solar cells, smart windows [1-3] and devices where optics of low thermal emissivity properties are required.

Indium tin oxide (ITO) material has received much attention due to its unique combined properties of transparency to visible light, high electrical conductivity and high IR reflectivity properties [4]. The only way to obtain good transparent conductors is to create electron degeneracy in a wide band gap (greater than 3 eV) oxide by controllably introducing non-stoichiometry and/or appropriate dopants [5] which in turn caused by oxygen vacancies and substitution of dopant created during film deposition [6].

Transport and optical properties of ITO films are highly sensitive to processing parameters, particularly, substrate temperature, film thickness, dopants, heat treatment (either annealing temperature or time), deposition pressure and other deposition conditions [4].

Several methods, such as sputtering [2] thermal evaporation [4, 7-8], pulsed laser deposition (PLD) [9-10], ion-beam assisted deposition [11], sol-gel [12-13], spray pyrolysis [14], and etc. have been followed for the deposition of ITO films on glass substrates.

Recently, silicon dioxide ( $\text{SiO}_2$ ) has attracted considerable attention because of the physicochemical properties, and its role in reducing the release of the toxic ions. These properties qualify it for many optoelectronic applications [15].

In this work we will study some of the optical and electrical properties of indium tin oxide thin films deposited onto a thin buffer layer of silicon dioxide at different substrate temperatures. The effect of thicknesses of buffer layer of  $\text{SiO}_2$  on the structure, optical and electrical properties of ITO/  $\text{SiO}_2$  films will be investigated too.

## 2. Experimental details

In the present work, appropriate ratios of highly pure (99.999%) of  $\text{In}_2\text{O}_3$  and  $\text{SnO}_2$  powder were ground separately by means of an agate mortar and pestle to prepare  $(\text{In}_2\text{O}_3)_{1-x}(\text{SnO}_2)_x$ . To insure complete mixing, the mixtures were grinded for at least 5 hours then; they were pressed in tablet form using a cold pressing technique.

In order to increase the diffusion process and consequently improve the homogeneity of the material, the tablet was heated up to  $900\text{ }^\circ\text{C}$  for 5 h in a muffle furnace, then the furnace was turned off until reaching the room temperature.

To avoid the substrate contamination, the glass substrates were ultrasonically cleaned by means of ultrasonic cleaner instrument model (T-9) using both acetone and carbon tetrachloride as solvents for 2 h and 1 h, respectively. Then, it was well washed by distilled water and left to dry in a muffle over at  $100\text{ }^\circ\text{C}$ .

A buffer layer of  $\text{SiO}_2$  with 0, 20, 40, 60 and 80 nm thick was deposited onto the ultrasonically clean silica glass substrates using Edward's high vacuum coating unit model E306A. Another layer of ITO with 200 nm thick was deposited onto the buffered layer at  $4 \times 10^{-6}$  mbar in the presence of oxygen. Every ITO thin film was deposited at certain substrate temperature as, 200, 250, 300, 350 and  $400\text{ }^\circ\text{C}$ . The source-to-substrate distance was fixed at 20 cm. The film thickness and deposition rate (5 nm/ min.) were controlled by means of a digital quartz crystal thickness monitor model TM200 Maxtek.

The transmittance  $T(\lambda)$  and reflectance  $R(\lambda)$  measurements were carried out using a double-beam JascoV-570 UV–VIS–NIR spectrophotometer (with photometric accuracy of  $\pm 0.002 - 0.004$  absorbance and  $\pm 0.3\%$  transmittance) over the wavelength range 200 – 2500 nm at normal incidence. Diffuse reflectance spectra were obtained using a diffuse reflectance accessory model ISN - 470, and the reflectance was converted by the instrument software to  $F(R)$  values according to the Kubelka–Munk method.

The electrical resistivity measurements were carried out using the two-terminal configuration by applying constant voltage to the sample and measuring the current through it using Keithley 614 electrometer.

The structural analysis was examined using an X-ray diffractometer (X' Pert Philips, Holland)  $\text{Cu-K}_\alpha$  radiation ( $\lambda=1.541838\text{ \AA}$ ) by varying diffraction angle  $2\theta$  from  $4$  to  $80^\circ$  by step width of  $0.04$ .

The chemical composition of the films was determined using energy dispersive analysis of X-ray (EDAX) using scanning electron microscope (Joel GSM 5300) attached with the EDAX unit.

## 3. Results and discussion

Fig. 1 shows the XRD diffraction patterns of the ITO films deposited onto two different kinds of substrates, one is glass substrate and the other is  $\text{SiO}_2$  coated glass with different  $\text{SiO}_2$  thicknesses.

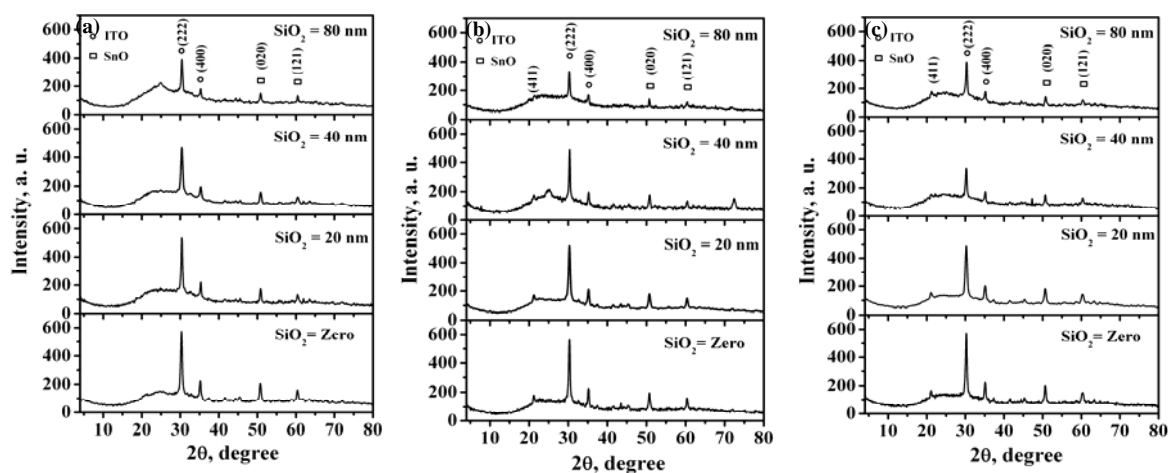


Fig. 1. X-ray diffraction patterns for ITO/SiO<sub>2</sub> films deposited at substrate temperature of 200 °C (a), 250 °C (b) and 325 °C (c) for different thicknesses of SiO<sub>2</sub> buffer layer.

Two diffraction peaks corresponding to (222) and (400) of ITO phase are observed at  $2\theta = 30.31$  and  $35.17^\circ$  respectively. Another two diffraction peaks corresponding to (020) and (121) of SnO phase are appeared at  $2\theta = 5.7$  and  $60.9^\circ$  respectively. The presence of SnO diffraction peaks indicates to the presence of oxygen vacancies. The diffraction peaks of both ITO and SnO are found to decrease with increasing the thickness of SiO<sub>2</sub> buffer layer in spite of increasing the substrate temperatures, which may be attributed to the substitution of either ITO or SnO by silicon atoms.

The grain sizes are estimated from the FWHM of the x-ray diffraction patterns and are found to decrease with increasing the thickness of the buffer layer thickness from 0 up to 40 nm for the considered substrate temperature 200, 250 and 325 °C. On the other side, the grain size are found to decrease with increasing the substrate temperature (200, 250 and 325 °C) except for thickness 0 and 80 nm at substrate temperatures 325 °C respectively as shown in Fig. 1 (d).

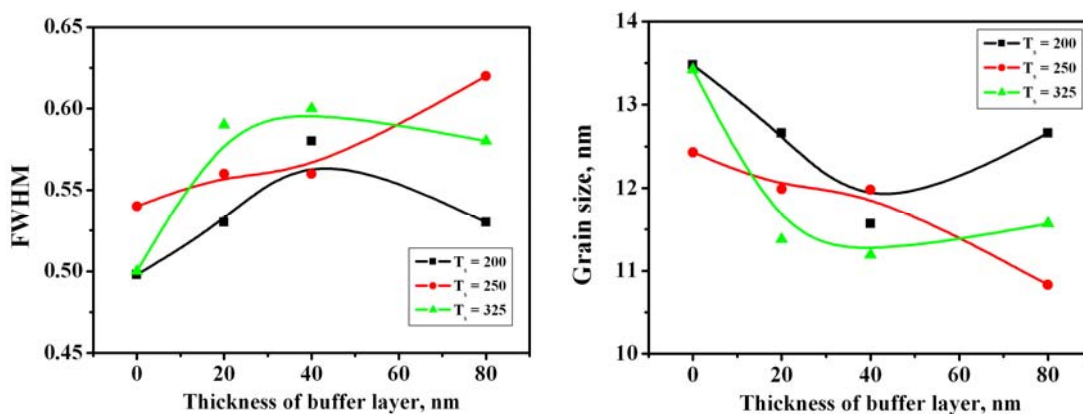


Fig. 1 (d) Variation of FWHM and grain size with thickness of buffer layer at certain substrate temperature.

The Edax diagrams of the prepared ITO bulk powder and ITO/SiO<sub>2</sub>/glass thin films are depicted in Figs.(2-a&b) respectively. (Fig.2-a) confirms qualitatively the presence of indium, tin and oxygen elements.

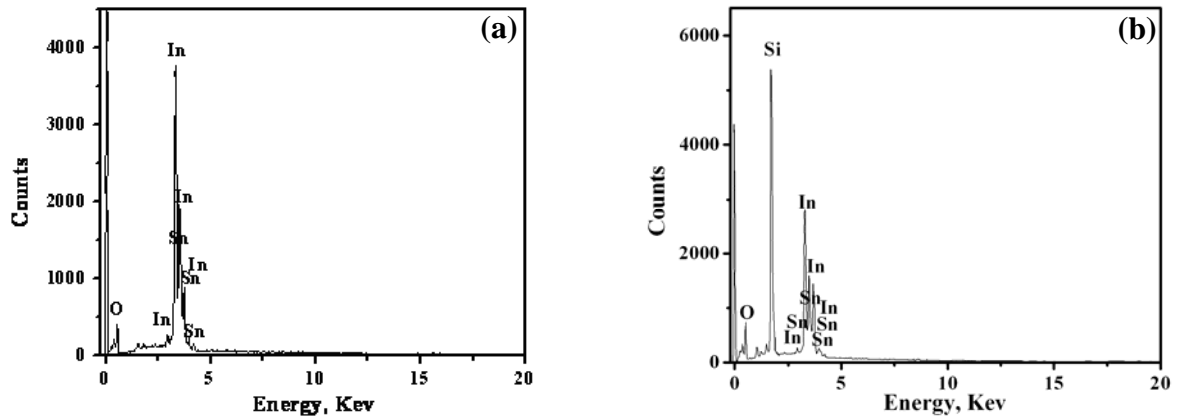


Fig. 2. EDAX diagram of ITO powder (a) and for ITO/ SiO<sub>2</sub>/ glass thin film (b)

This analysis shows that the atomic percentage are, In (51.33 %), Sn (6.58 %) and O (42.09 %). Fig. (2-b) verifies that the atomic percentage of Si, In, Sn and O are (41.10%), (18.74%), (6.21%) and (33.94%) respectively. This feature illustrates the good quality of ITO/SiO<sub>2</sub> thin films deposited by electron beam evaporation technique.

The optical transmittance spectra of ITO/SiO<sub>2</sub> thin films with different thicknesses of SiO<sub>2</sub> buffer layer prepared at different substrate temperatures are shown in Fig. 3. The optical transmittance increases with increasing SiO<sub>2</sub> buffer layer thickness as shown in Fig. (3-a & b & f).

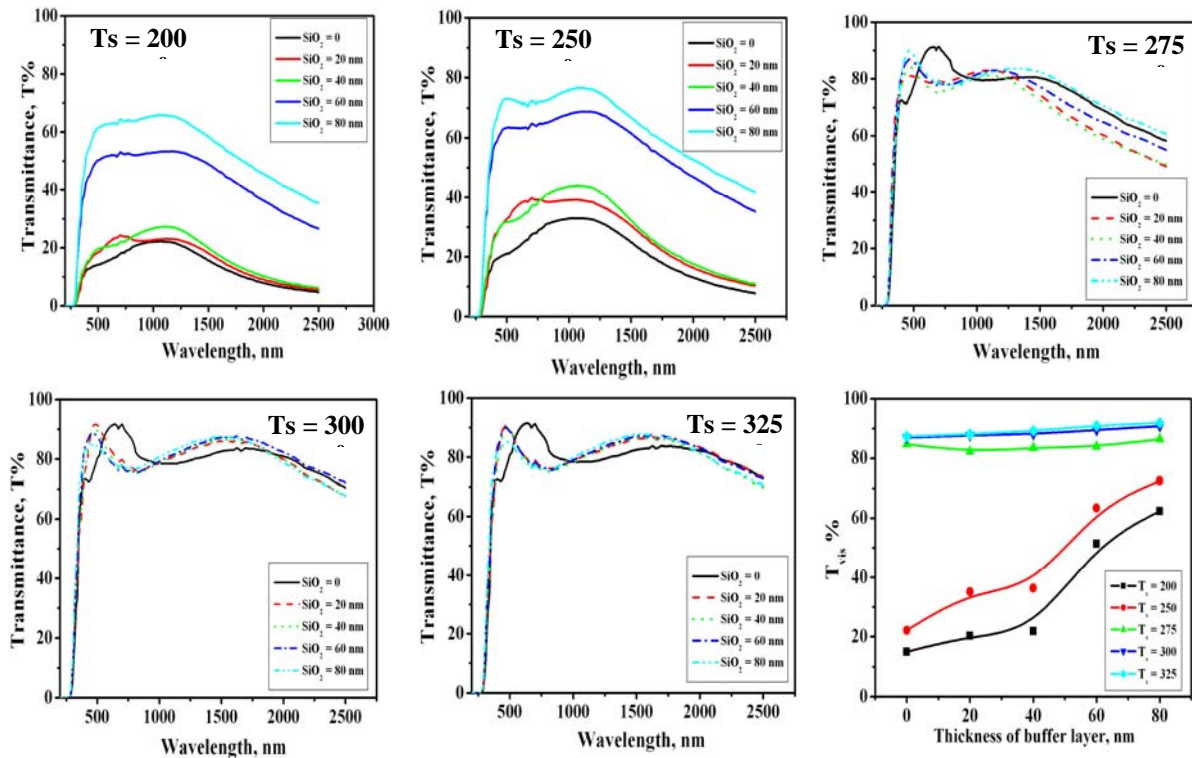


Fig. 3. The transmittance spectra of ITO films deposited at different substrate temperatures onto different thicknesses of SiO<sub>2</sub> buffer layer and the variation of the average transmittance in the visible region with the thickness of buffer layer.

In addition, the average transmittance values in the visible region varies between 15-73% whereas those in the near infrared region changes between 10-56%. As shown in Figs.(3-c&d&e), the transmittance increases with increasing the SiO<sub>2</sub> buffer layer reaching 92 % in the visible region and 83% in the near infrared (NIR) region of the spectrum.

The typical UV-VIS –NIR optical reflectance spectra of ITO/SiO<sub>2</sub> thin films with different thicknesses of SiO<sub>2</sub> buffer layer prepared at different substrate temperatures are shown in Fig. 4. It is evident that the reflectance decreases with increasing the thickness of buffer layer of the SiO<sub>2</sub> in the NIR region for films deposited at different substrate temperatures. It is observed also that the optical reflectance decreases with increasing the substrate temperature. The decrease in reflection of the ITO/SiO<sub>2</sub> films deposited at different substrate temperature with increasing the thickness of buffer layer temperature of the SiO<sub>2</sub> buffer layer can be attributed to the decrease of the surface roughness of the films, which in turn depends on the particle size [16].

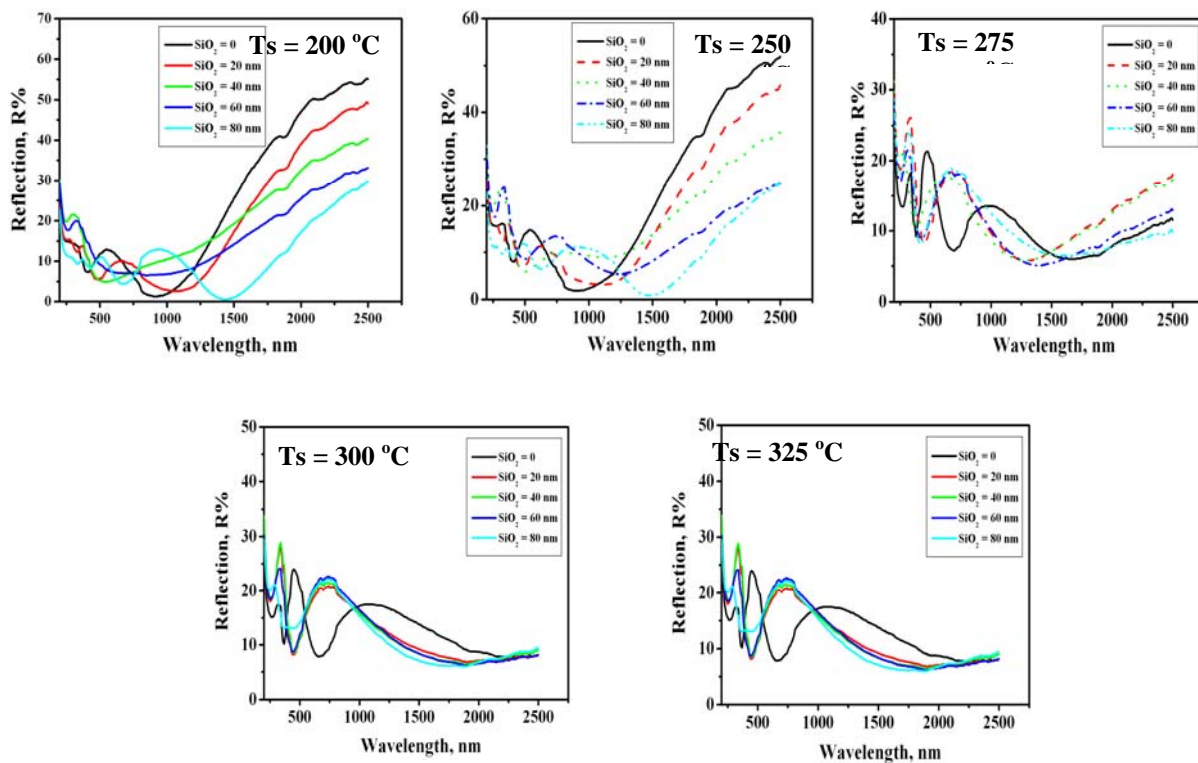


Fig. 4. The reflection spectra of ITO films deposited at different substrate temperatures onto different thicknesses of SiO<sub>2</sub> buffer layer

The unwanted heat radiation called thermal emissivity of ITO deposited films at different substrate temperatures on a buffer layer of SiO<sub>2</sub> with different thicknesses is determined using the following eqn.[17]:

$$\epsilon_d = 1 - T_{IR} - R_{IR}$$

Figure 5 shows the substrate temperature dependence of thermal emissivity for films with different thicknesses of SiO<sub>2</sub> buffer layer. It is clear that the thermal emissivity decreases with increasing the substrate temperature for all films deposited onto a different thickness of SiO<sub>2</sub> buffer layer. This decrease is attributed to the decrease of reflectivity in the near infrared region.

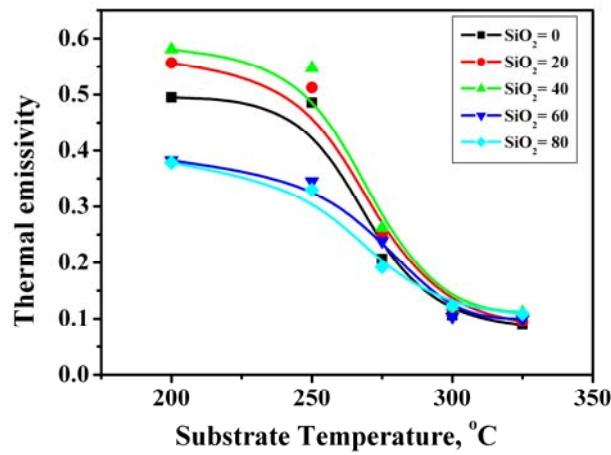


Fig. 5. The substrate temperature dependence of the thermal emissivity of ITO films deposited onto different thicknesses of  $\text{SiO}_2$  buffer layer.

Fig. 6 shows the diffuse reflectance spectra of ITO/  $\text{SiO}_2$  films extracted from the Kubelka–Munk (KM) theory which is proportional to the optical absorption coefficient [18]. For ITO/  $\text{SiO}_2$  thin film deposited at different substrate temperature, it is seen that, increasing the thickness of  $\text{SiO}_2$  results in shifting the peaks which are lying in the visible region toward shorter wavelength. This indicates to the shift in the absorption edge to shorter wavelength and to an increase in the energy gap due to the decrease of the particle size [19] which is in agreement with Fig. 1(d). The change in the fundamental absorption edge reflects the density variation and the short-range structural modifications [20]. It is shown also that the diffuse reflectance of ITO/ $\text{SiO}_2$  thin film decrease with increasing either the thickness of buffer layer and/or the substrate temperature, indicating to the decrease of scattering coefficient. This decrease of the diffuse reflectance can be ascribed to the decrease in the grain size and film roughness [21] which is documented by Fig. 1(d).

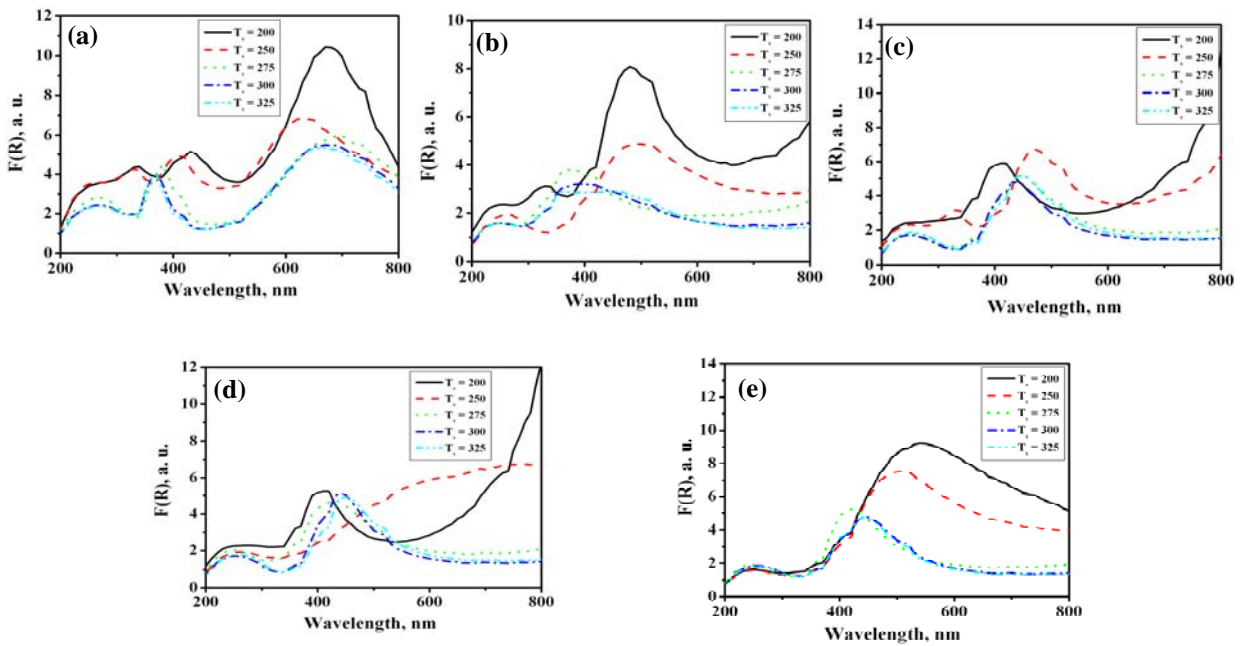


Fig. 6. Plots of  $F(R)$  vs. wavelength of ITO thin films deposited onto a buffer layer of  $\text{SiO}_2$  with thicknesses of 0 (a), 20 (b), 40 (c), 60 (d) and 80 nm (e) at different substrate temperatures.

Table 1 shows the average refractive index dependence of substrate temperature. It is shown that the refractive index increases with increasing the substrate temperature. This increase can be ascribed to the increase in the carrier concentration [4].

Table 1: values of refractive index ( $n$ ) measured at different substrate temperature for certain buffer layer thickness.

Substrate temperature	$n$ [ $\text{SiO}_2 = 0$ ]	$n$ [ $\text{SiO}_2 = 20$ ]	$n$ [ $\text{SiO}_2 = 40$ ]	$n$ [ $\text{SiO}_2 = 60$ ]	$n$ [ $\text{SiO}_2 = 80$ ]
200	1.77	1.80	1.94	1.75	1.69
250	1.91	1.90	2.13	1.90	1.85
<b>275</b>	2.13	2.32	2.30	2.28	2.27
<b>300</b>	2.19	2.41	2.46	2.43	2.41
<b>325</b>	2.20	2.43	2.48	2.45	2.43

The dependence of the optical gap on both the buffer layer thickness and the substrate temperature are demonstrated in Fig. 7 bearing in mind that the optical gaps of the films are determined by extrapolating the linear portion of the plots of  $(\alpha h\nu)^2$  versus  $h\nu$ . Fig. 7 shows that the optical gaps increase with increasing both of the substrate temperature and the thickness of  $\text{SiO}_2$  buffer layer. The increase of the optical gaps ( $E_g$ ) is attributed to the decrease of the particle size [19].

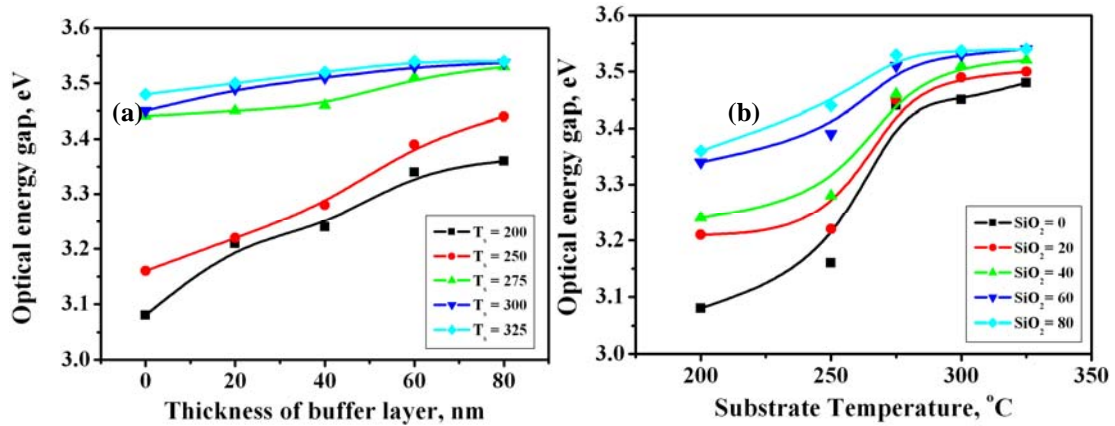


Fig. 7. Variations of the optical energy gap with thickness of buffer layer (a) and with substrate temperature (b).

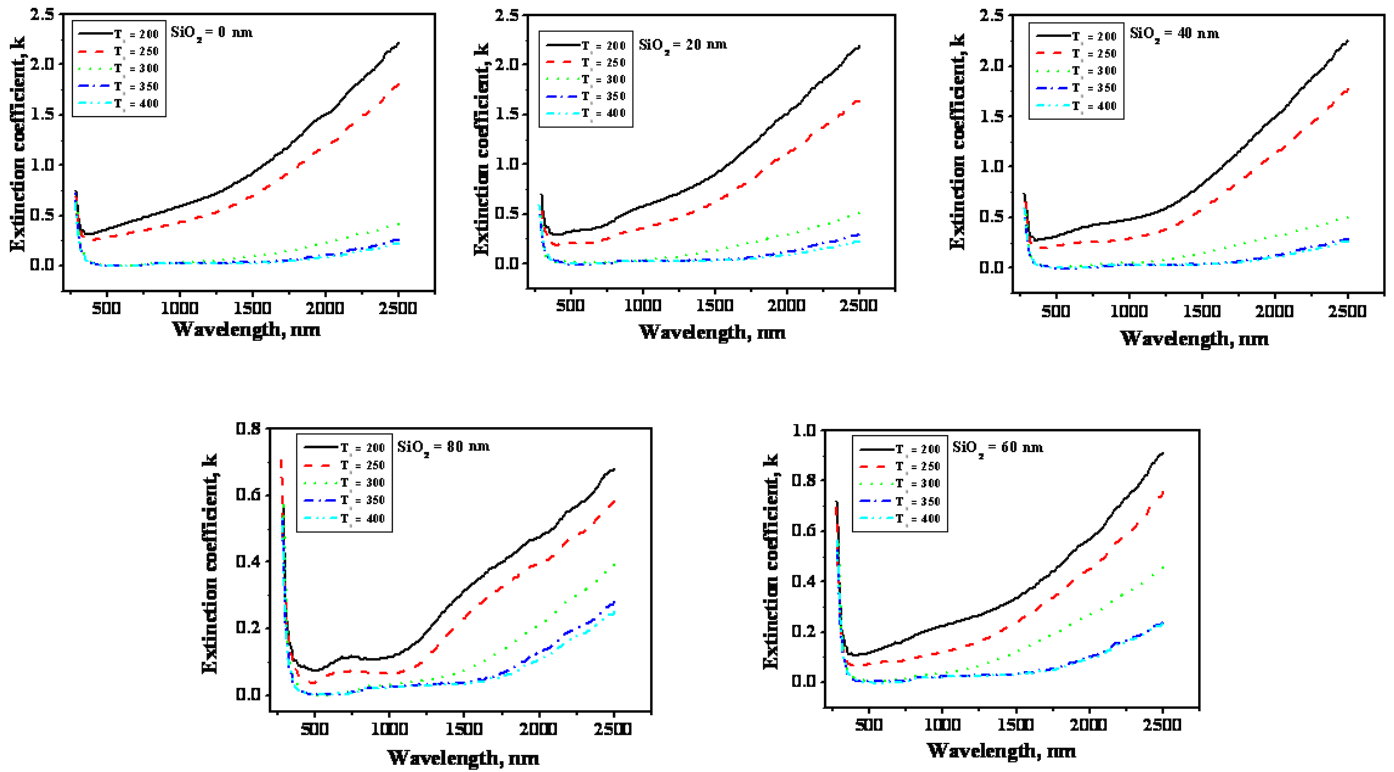


Fig. 8. Variations of the extinction coefficient with wavelength of ITO films deposited at different substrate temperatures onto different thicknesses of  $\text{SiO}_2$  buffer layer.

It is seen that the extinction coefficient decreases with increasing the substrate temperature and/or the increase of the thickness of buffer layer as shown in Fig. 8. The decrease of the extinction coefficient can be attributed to the decrease of absorption coefficient ( $\alpha$ ), where  $k = \alpha\lambda/4\pi$ . Fig. 9 shows the variations of the film resistivity with the substrate temperature for all films deposited onto different thicknesses of  $\text{SiO}_2$  buffer layer. The resistivity decreases with increasing the substrate temperature up to 275 °C, then it increases gradually with further increasing in the substrate temperature. On the other hand the resistivity increases with increasing the thickness of the  $\text{SiO}_2$  buffer layer for films deposited at substrate temperature of 200 and 250 °C. At substrate temperature of 275 °C the value of resistivity for all film with different thickness of buffer layers are almost has a lower value. Above substrate temperature of 275 °C the resistivity decreases gradually with further increase of the buffer layer thickness.

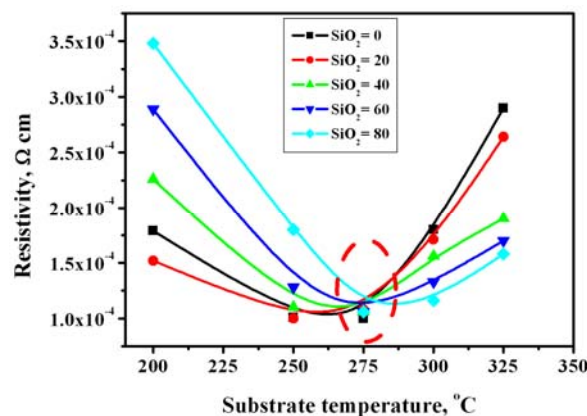


Fig.9 The substrate temperature dependence of electrical resistivity of ITO films deposited onto different thicknesses of  $\text{SiO}_2$  buffer layer.

The decrease of resistivity of deposited films at substrate temperature up to 275 °C can be attributed to the presence of SnO phase (as shown in Fig. 1), indicating the presence of oxygen vacancies during deposition. On the other hand, the increase of resistivity at higher substrate temperature can be ascribed to the substitution of some atoms of Sn with Si atoms that created during film deposition or due to the crystalline behavior.

#### 4. Conclusion

The obtained results of the present work reveal that:

- Decreasing the grain size results in decreasing the reflectance and thermal emissivity of the considered films, whereas the optical gap increases.
- The optical transmittance increases with increasing the thickness of SiO<sub>2</sub> buffer layer. A transmittance value of 92 % in the visible region and 83% in the near infrared (NIR) region of the spectrum are obtained for deposited ITO films at substrate temperature of 325 °C onto a buffer layer of SiO<sub>2</sub> with 80 nm thick
- The thermal emissivity of ITO films deposited at different substrate temperatures on a buffer layer of SiO<sub>2</sub> with different thicknesses are found to decrease with increasing the substrate temperature.
- The extinction coefficient decreases with increasing the substrate temperature and/or the increase of the thickness of buffer layer.
- The diffuse reflectance of ITO/SiO<sub>2</sub> thin film decrease with increasing either the thickness of buffer layer and/or the substrate temperature, indicating to the decrease of scattering coefficient.
- A decrease of the average refractive index is observed with increasing the substrate temperature.
- The optical gap increases with increasing both of the substrate temperature and the thickness of SiO<sub>2</sub> buffer layer
- The electrical resistivity decreases with increasing the substrate temperature up to 275 °C, and then it was increased gradually with further increasing in the substrate temperature. A resistivity value of  $1 \times 10^{-4} \Omega \text{ cm}$  has been obtained for deposited films at 275 °C

#### References

- [1] T. Neubert, F. Neumann a, K. Schiffmann a, P. Willich a, A. Hangleiter, *Thin Solid Films* **513**, 319 (2006)–324
- [2] Jaehyeong Lee , Hakkee Jung, Jongin Lee, Donggun Lim, Keajoon Yang, Junsin Yi, Woo-Chang Song, *Thin Solid Films* **516**, 1634 (2008).
- [3] D. Dimos, W.L. Warren, M.B. Sinclair, B.A. Tuttle, R.W. Schwartz, *J. Appl. Phys.* **76**, 4305 (1994).
- [4] H.M. Ali, H.A. Mohamed, and S.H. Mohamed, *Eur. Phys. J. Appl. Phys.* **31**, 87 (2005)
- [5] K. L. CHOPRA, S. MAJOR AND D. K. PANDYA, *Thin Solid Films*, **102**, 1 (1983).
- [6] D. Beena, K.J. Lethy, R. Vinodkumar, V.P. Mahadevan Pillai, *Solar Energy Materials & Solar Cells* **91**, 1438 (2007).
- [7] H. M. Ali, *phys. stat. sol. (a)* **202**(14), 2742 (2005).
- [8] J.L. Yao, S. Hao, J.S. Wilkinson, *Thin Solid Films* **189**, 227 (1990).
- [9] C. Viespe, C. Grigoriu, M. Popescu, F. Sava, A. Lőrinczi, A. Velea, S. Zamfira, *J. Optoelectron. Adv. Mater.* **9**(11), 3563 (2007).
- [10] Fernande Fotsa-Ngaffo, Anna Paola Caricato, Francesco Romano, *Applied Surface Science* **255**, 9684 (2009).
- [11] Zhinong Yu, Yu-qiong Li, Fang Xia, Wei Xue, *Surface & Coatings Technology* **204**, 131 (2009).
- [12] Jung Kyun Kim, Yong Gyu Choi, *Thin Solid Films* **517**, 5084 (2009).
- [13] Jung-Min Lee, Byung-Hyun Choi, Mi-Jung Ji, Yong-Tae An, Jung-Ho Park, Jae-Hong Kwon,

- Byeong-Kwon Ju, *Thin Solid Films* **517**, 4074 (2009).
- [14] H. Haitjema and J. J. P. Elich, *Thin Solid Films* **205**, 93 (1991).
- [15] Mao-Quan Chu, Ye Sun, Xiao-Yan Shen, Guo-Jie Liu, *Physica E* **35**, 75 (2006).
- [16] H. M. Ali, H. A. Mohamedy, M. M. Wakkad, and M. F. Hasaneen, *Japanese Journal of Applied Physics* **48**, 041101 (2009).
- [17] P.K. Biswas, A. De, N.C. Pramanik, P.K. Chakraborty, K. Ortnerb, V. Hockb, S. Korder, *Materials Letters* **57**, 2326 (2003).
- [18] B. Hapke, *Theory of Reflectance and Emittance Spectroscopy*, Cambridge University Press, 2003.
- [19] M. Bellardita, M. Addamo, A. Di Paola, L. Palmisano, *Chemical Physics* **339**, 94 (2007).
- [20] Fernande Fotsa-Ngaffo, Anna Paola Caricato, Francesco Romano, *Applied Surface Science* **255**, 9684 (2009).
- [21] M.S. Rafique, M. Khaleeq-ur-Rahman, Saif-ur-Rehman, Safia Anjum, M. Shahbaz Anwar, K.A. Bhatti, Saba Saeed, M.S. Awan, *Vacuum* **82**, 1233 (2008).